Reconstruction of phonon dispersion in Si nanocrystals

2002 J. Phys.: Condens. Matter 14 L671

(http://iopscience.iop.org/0953-8984/14/41/101)

INSTITUTE OF PHYSICS PUBLISHING JOURNAL OF PHYSICS: CONDENSED MATTER

J. Phys.: Condens. Matter **14** (2002) L671–L677 PII: S0953-8984(02)39487-6

LETTER TO THE EDITOR

Reconstruction of phonon dispersion in Si nanocrystals

Xinhua Hu and Jian Zi[1]

Surface Physics Laboratory (National Key Laboratory), Fudan University, Shanghai 200433, People's Republic of China

E-mail: jzi@fudan.edu.cn

Received 15 July 2002
Published 4 October 2002
Online at stacks.iop.org/JPhysCM/14/L671

Abstract

A theoretical approach is developed for reconstructing phonon dispersion in Si nanocrystals. It is found that for Si nanocrystals with size larger than 2 nm, smeared phonon dispersion could be established. The evolution of nanocrystal phonons into bulk ones is studied. Frequency shifts of bulk-like phonons versus nanocrystal size are calculated.

Semiconductor nanocrystals, also known as quantum dots, exhibit a number of novel and interesting properties that have not been observed in bulk materials [1, 2]. In nanocrystals, motions of electrons and phonons are confined in all three spatial dimensions. Consequently, the energies and wavefunctions of electrons or phonons in nanocrystals are considerably modified compared to their counterparts in the corresponding crystalline phases due to the finite-size effects. As a result, many physical properties such as carrier relaxations, Raman scattering, luminescence, electron–phonon interactions, and exciton–phonon interactions will be altered significantly [3–10]. To explain the interesting phenomena associated with such processes in nanocrystals, bulk phonon dispersion relations have been used in many studies. For instance, a phenomenological phonon confinement model, in which the bulk phonon dispersion is used, has been widely adopted to calculate the Raman scattering from optical phonons in semiconductor nanocrystals [11–13]. To study optical properties in polar semiconductor nanocrystals, the Fröhlich electron–phonon interactions were calculated either using a dielectric model [14] or using a macroscopic continuum model [15], in which a dispersionless relation or a bulk dispersion relation was used. Therefore, it is desirable to obtain the phonon dispersion in nanocrystals, from which many interesting phenomena in nanocrystals could be elucidated more readily.

Phonon dispersion only exists in infinite crystals. For very small nanocrystals such as molecules or clusters, phonon dispersion should be expected to be ill defined. However, with

[1] Author to whom any correspondence should be addressed.

increasing nanocrystal size, phonon dispersion will eventually be established. From this simple argument, one can conjecture that phonon dispersion in nanocrystals might exist, although in *smeared* form.

In the letter, we propose a theoretical approach for reconstructing the smeared phonon dispersion in nanocrystals. The central idea is the following. For infinite crystals, the phonon dispersion $\omega_n(\boldsymbol{k})$ is well defined and has a single value for each $\boldsymbol{k}$ and n, where $\boldsymbol{k}$ is the wavevector and n is the band index. On the other hand, the phonon dispersion in nanocrystals is not well defined due to the lack of translational symmetry. However, wavefunctions of phonons in a nanocrystal can be expanded as a linear combination of the vibrational Bloch waves of the corresponding infinite crystal, described by wavevectors in the Brillouin zone [16]. Then, a nanocrystal phonon mode is viewed as contributions from many bulk phonon modes. For a given $\boldsymbol{k}$, $\omega_n(\boldsymbol{k})$ is no longer a single value. It has a distribution over the frequency domain, leading to the smeared phonon dispersion.

In the present work, we use Si nanocrystals as an example and reconstruct the phonon dispersion, even though it is of smeared form. In our calculations, Si nanocrystals are modelled by spherical bulk-terminated Si clusters saturated by hydrogen atoms. We use the same force constants for Si nanocrystals as were used for bulk Si, obtained by a partial density approach [17]. Such microscopic lattice dynamical calculations have been successfully carried out to study Raman scattering from optical and acoustic phonons in Si nanocrystals and thermodynamical properties of Si nanocrystals [18–21].

Mathematically, the eigenfunctions of either electrons or phonons in a nanocrystal can be expressed as superpositions of a set of orthogonal and complete basis functions. In our studies, a set of plane waves are adopted, which satisfy the following orthogonality and completion conditions:

$$\sum_{\boldsymbol{R}} \mathrm{e}^{\mathrm{i}(\boldsymbol{k}-\boldsymbol{k}')\cdot\boldsymbol{R}} = N\delta_{\boldsymbol{k},\boldsymbol{k}'}, \tag{1}$$

$$\sum_{\boldsymbol{k}} \mathrm{e}^{\mathrm{i}(\boldsymbol{R}-\boldsymbol{R}')\cdot\boldsymbol{k}} = N\delta_{\boldsymbol{R},\boldsymbol{R}'}, \tag{2}$$

where N is the number of allowable wavevectors $\boldsymbol{k}$ and $\boldsymbol{R}$ are the face-centred cubic (fcc) lattice vectors. To satisfy the above conditions, the fcc lattice vector $\boldsymbol{R}$ must be confined to a cube with a length of Ma, where a is the lattice constant and M is an integer. Moreover, the wavevectors can only take the values $k = 2\pi/Ma(n_1, n_2, n_3)$ and have to be located in the Brillouin zone of bulk Si, where $n_{1,2,3}$ are integers. N and M satisfy the relation $N = 4M^3$.

To carry through the idea discussed above, a Si nanocrystal is placed into the cube, the length of which is just the diameter of the nanocrystal. For the cube, the vibrational eigenfunctions are given by

$$\boldsymbol{F}_i(\boldsymbol{R},\kappa) = \begin{cases} \boldsymbol{u}_i(\boldsymbol{R},\kappa) & \text{if } \boldsymbol{R} \in \text{dot}, \\ 0 & \text{if } \boldsymbol{R} \notin \text{dot}, \end{cases} \tag{3}$$

where $\kappa = 1, 2$ is the atom index in the primitive unit cell of the fcc lattices, i is the mode index of a nanocrystal, and $\boldsymbol{u}_i(\boldsymbol{R},\kappa)$ are the vibrational eigenfunctions of the nanocrystal. The functions $\boldsymbol{F}_i(\boldsymbol{R},\kappa)$ can then be expressed as a superposition of the set of plane waves discussed above, given by

$$\boldsymbol{F}_i(\boldsymbol{R},\kappa) = \sum_{\boldsymbol{k}} \boldsymbol{A}_i(\boldsymbol{k},\kappa)\mathrm{e}^{\mathrm{i}\boldsymbol{k}\cdot\boldsymbol{R}}, \tag{4}$$

where the $\boldsymbol{A}_i(\boldsymbol{k},\kappa)$ are the expansion coefficients, obtained from

$$\boldsymbol{A}_i(\boldsymbol{k},\kappa) = \frac{1}{N}\sum_{\boldsymbol{R}} \boldsymbol{F}_i(\boldsymbol{R},\kappa)\mathrm{e}^{-\mathrm{i}\boldsymbol{k}\cdot\boldsymbol{R}}. \tag{5}$$

The projected vibrational density of states (VDOS) of a given atom $(\boldsymbol{R}, \kappa)$ in the nanocrystal can be calculated; it is given by

$$\rho_\omega(\boldsymbol{R}, \kappa) = \sum_i |\boldsymbol{F}_i(\boldsymbol{R}, \kappa)|^2 \, \delta(\omega - \omega_i). \tag{6}$$

This VDOS is considered in real space. It can be also considered in wavevector space, where it is given by

$$\rho_{\boldsymbol{k}}(\omega) = \sum_i P_{i\boldsymbol{k}} \delta(\omega - \omega_i). \tag{7}$$

This is the projected VDOS over a certain wavevector. The quantity $P_{i\boldsymbol{k}}$ is defined by

$$P_{i\boldsymbol{k}} = \sum_\kappa |\boldsymbol{A}_i(\boldsymbol{k}, \kappa)|^2 . \tag{8}$$

It can be shown that for the infinite crystal, $\rho_{\boldsymbol{k}}(\omega)$ is exactly the projected VDOS for a fixed wavevector. The definition of the quantity $P_{i\boldsymbol{k}}$ has other advantages. The projected VDOS of a given mode in the nanocrystal can be derived from $P_{i\boldsymbol{k}}$, given by

$$\rho_i(\omega) = \sum_{\boldsymbol{R},\kappa} |\boldsymbol{u}_i(\boldsymbol{R}, \kappa)|^2 \, \delta(\omega - \omega_i) = \sum_{\boldsymbol{k}} P_{i\boldsymbol{k}} \delta(\omega - \omega_i), \tag{9}$$

and the derived total VDOS is

$$\rho(\omega) = \sum_{i,\boldsymbol{k}} P_{i\boldsymbol{k}} \delta(\omega - \omega_i). \tag{10}$$

In all of the following calculations of the VDOS, the delta function is broadened by using a Lorentzian function with the broadening coefficient chosen to be 4 cm^{-1}.

In figure 1 the projected VDOS for a Si nanocrystal of size 2.21 nm consisting of 281 Si atoms at some special $\boldsymbol{k}$-points in the Brillouin zone is given. The bulk modes are indicated by vertical arrows. By inspecting the vibrational patterns and analysing the expansion coefficients, we can classify nanocrystal modes according to the similarity to the bulk modes. It is obvious that there are well-defined peaks in the projected VDOS in the Si nanocrystal. Some peaks are smeared compared to those for the bulk. The well-defined peaks are shifted in frequency with respect to the bulk modes. Moreover, extra peaks with small intensity appear in the nanocrystal.

At the Γ point, for the bulk, two transverse optical (TO) modes and one longitudinal optical (LO) mode are triply degenerate. For the Si nanocrystal, near the bulk optical modes, there is a sharp peak, whose frequency is lower than that of the bulk optical modes. By inspecting the vibrational patterns, it is found that this peak is derived from the bulk LO phonon. It is a LO-like phonon. The downward shifting in frequency can be understood by considering confinement effects, since the bulk LO dispersion for Si decreases with increasing wavevector. On the lower-frequency side of this peak, there is a small peak, attributable to the TO-like mode. The triple degeneracy of the LO and TO modes at the Γ point in the bulk is lifted in the nanocrystal due to the finite-size effects. Extra peaks with small intensity, which do not exist for the bulk, appear for the nanocrystal. These modes have no obvious bulk parentage. By inspecting the vibrational eigenfunctions of the nanocrystal, it is found that the vibrations of these modes are mostly localized near the surface region. These modes are surface modes in nature.

At the X point, the very smeared peak on the low-frequency side is derived from the doubly degenerate transverse acoustic (TA) modes of the bulk. The highest peak on the high-frequency side corresponds to the doubly degenerate TO modes of bulk. On the lower-frequency side of this peak, a series of smeared peaks exist. These peaks are derived from the degenerate LA and LO modes of the bulk. Peaks on the higher-frequency side have more parentage from the

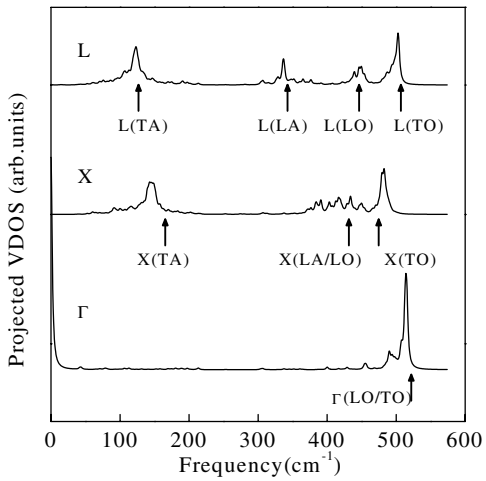

Figure 1. Projected VDOS at the Γ, X, and L points in the Brillouin zone for a Si nanocrystal. The size of this nanocrystal is 2.21 nm; it consists of 281 Si atoms. Bulk modes are indicated by vertical arrows.

bulk LO mode, while peaks on the lower-frequency side have more parentage from the bulk LA mode. Obviously, the double degeneracy of the LA and TO modes at the X point in the bulk is lifted.

At the L point, the smeared peak on the low-frequency side is attributed to the TA-like modes. The peak with the highest frequency is derived from the bulk TO modes. The two broad peaks in between are found to originate from the bulk LA and LO phonons, respectively.

In the above discussions, it is found that with respect to those for the bulk, some peaks for nanocrystals are shifted in frequency, some are broadened significantly, and some extra peaks appear. With increase in nanocrystal size, the bulk-like peaks of the nanocrystals can be expected to shift towards bulk mode peaks, evolving finally into bulk phonon peaks. The broadened peaks will become sharper and the extra peaks will disappear. Therefore, the projected VDOS $\rho_{\boldsymbol{k}}(\omega)$ contains essential information on phonon evolution.

In figure 2 the projected VDOS $\rho_{\boldsymbol{k}}(\omega)$ for Si nanocrystals with different sizes, over $\boldsymbol{k}$-points in the Brillouin zone, is plotted for rebuilding the phonon dispersion. In the infinite crystal, for every $\boldsymbol{k}$-point, the bulk phonon modes correspond to sharp peaks in the spectra of the projected VDOS $\rho_{\boldsymbol{k}}(\omega)$. Normally, six peaks will be found owing to the fact that there are two atoms in the primitive unit cell for bulk Si. For some symmetrical points or directions, there may be less than six peaks due to degeneracy.

It can be seen from the figure that for small Si nanocrystals, most of the peaks in the projected VDOS are very smeared, leading to an ill-defined phonon dispersion. But with increase in the nanocrystal size, the peaks become sharper and resemble more those of bulk modes. It is found that for Si nanocrystals with size larger than 2 nm, phonon dispersion in nanocrystals is established little by little. The evolutions of nanocrystal phonons into bulk ones are different for modes with different wavevectors and frequencies. Generally, it seems that high-frequency modes in nanocrystals evolve faster than low-frequency modes since the peaks at high frequencies are sharper than those at low frequencies. This can be understood by considering the fact that the wavelengths of low-frequency modes are larger than those of high-frequency modes. For a nanocrystal, nanocrystal modes with higher frequencies will 'view' more wavelengths than those with lower frequencies. It is also found that highly

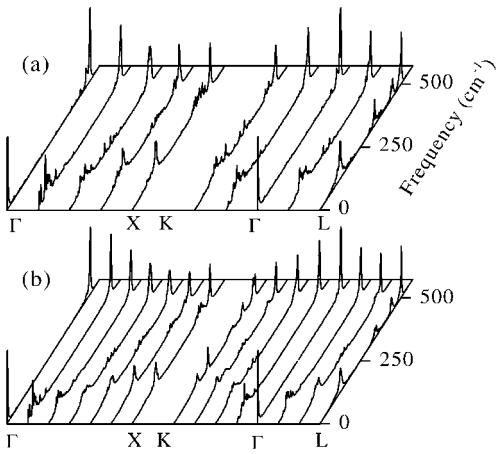

Figure 2. A three-dimensional plot for the projected VDOS over wavevectors along the [100] (ΓX), [110] (ΓKX), and [111] (ΓK) directions for Si nanocrystals with sizes of (a) 2.21 nm and (b) 3.27 nm, consisting of 281 and 915 Si atoms, respectively. The vertical axis indicates the amplitudes of the projected VDOS in arbitrary units.

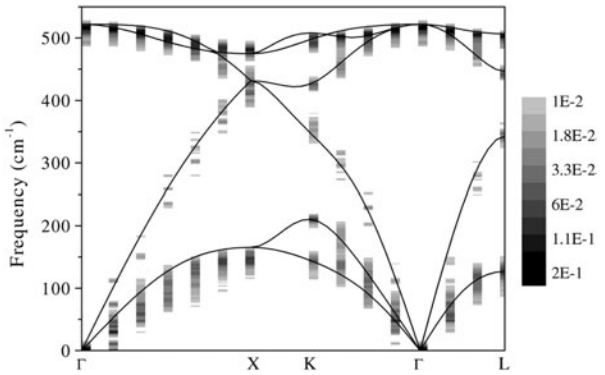

Figure 3. A contour plot of the projected VDOS over wavevectors in the Brillouin zone for a Si nanocrystal of size 3.27 nm consisting of 915 atoms. Solid curves are bulk dispersion curves.

symmetrical modes (with highly symmetrical wavevectors) evolve faster than low-symmetry modes. This can be understood by considering the fact that for high-symmetry modes, on inspecting the vibrational patterns, it is found that vibrations are more confined to the central region of nanocrystals, while vibrations for low-symmetry modes are concentrated more in the surface region.

To characterize and classify nanocrystal modes, the projected VDOS in a Si nanocrystal of size 3.27 nm is plotted as a contour graph over the Brillouin zone, together with the bulk phonon dispersion, in figure 3. The greyscale indicates the amplitudes of the projected VDOS. The sharper and the darker a peak is, the more similar to a bulk mode peak it is. The qualitative conclusions reached above are clearly supported by the figure.

From the reconstructed phonon dispersion for the nanocrystals, we can identify the characteristics of nanocrystal modes according to the similarity to the bulk modes. Due to the finite-size effects, bulk-like modes will shift in frequency with respect to their bulk

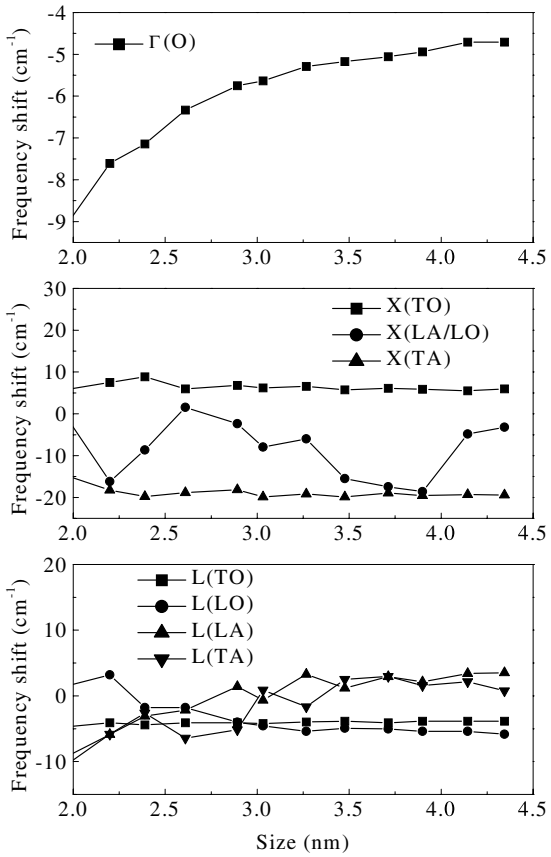

Figure 4. Frequency shifts of some bulk-like modes in Si nanocrystals with respect to their bulk counterparts versus nanocrystal size.

counterparts. In figure 4, frequency shifts for some modes in nanocrystals with respect to their bulk versions versus size are given. It can be seen from the figure that the frequency shifts of optical phonons are in general smaller than those of acoustic phonons, indicating again that optical phonons evolve faster than acoustic phonons.

In summary, we have proposed a theoretical approach for reconstructing phonon dispersion in Si nanocrystals. By inspecting the vibrational patterns and by analysing the expansion coefficients, phonons in Si nanocrystals can be classified according to the origination from the bulk modes. We found that for nanocrystals with size larger than 2 nm, smeared phonon dispersion could be established. The evolutions of nanocrystal phonons into bulk ones are different for different frequencies and different wavevectors in the Brillouin zone. The frequency shifts of nanocrystal phonons with respect to their bulk counterparts versus nanocrystal size were calculated.

This work was supported in part by the National Natural Science of Foundation of China. Interesting discussion with Professor S-L Zhang is acknowledged.

References

[1] Brus L 1991 *Appl. Phys.* A **53** 465
[2] Alivisatos A P 1996 *Science* **271** 933
[3] Krauss T D and Wise F W 1997 *Phys. Rev. Lett.* **79** 5102
[4] Baranov A V, Yamauchi S and Masumoto Y 1997 *Phys. Rev.* B **56** 10332
[5] Itoh T, Nishijima M, Ekimov A I, Gourdon C, Efros Al L and Rosen M 1995 *Phys. Rev. Lett.* **74** 1645
[6] Inoshita T and Sakaki H 1997 *Phys. Rev.* B **56** R4355
[7] Scamarcio G, Spagnolo V, Ventruti G, Lugara M and Righini G C 1996 *Phys. Rev.* B **53** R10489
[8] Mishra P and Jain K P 2001 *Phys. Rev.* B **64** 073304
[9] Urayama J, Norris T B, Singh J and Bhattacharya P 2001 *Phys. Rev. Lett.* **86** 4930
[10] Krauss T D and Wise F W 1997 *Phys. Rev.* B **55** 9860
[11] Richter H, Wang Z P and Ley L 1981 *Solid State Commun.* **39** 625
[12] Campbell I H and Fauchet P M 1986 *Solid State Commun.* **58** 739
[13] Münder H, Andrzejak C, Berger M G, Klemradt U, Lüth H, Herino R and Ligeon M 1992 *Thin Solid Films* **221** 27
[14] Klein M C, Hache F, Ricard D and Flytzanis C 1990 *Phys. Rev.* B **42** 11123
[15] Roca E, Trallero-Giner C and Cardona M 1994 *Phys. Rev.* B **49** 13704
[16] Fu H, Ozoliņš V and Zunger A 1999 *Phys. Rev.* B **59** 2881
[17] Falter C 1988 *Phys. Rep.* **164** 1
[18] Zi J, Büscher H, Falter C, Ludwig W, Zhang K and Xie X 1996 *Appl. Phys. Lett.* **69** 200
[19] Zi J, Zhang K and Xie X 1997 *Phys. Rev.* B **55** 9263
[20] Zi J, Zhang K and Xie X 1998 *Phys. Rev.* B **58** 6712
[21] Hu X, Wang G, Wu W, Jiang P and Zi J 2001 *J. Phys.: Condens. Matter* **13** L835